

# Circumventing resistance within the Ewing sarcoma microenvironment by combinatorial innate immunotherapy

Wen Luo,<sup>1,2</sup> Hai Hoang,<sup>1</sup> Hongwen Zhu,<sup>1</sup> Katherine Miller,<sup>3,4</sup> Xiaokui Mo,<sup>5</sup> Shiori Eguchi,<sup>1</sup> Meijuan Tian,<sup>1</sup> Yanling Liao,<sup>1</sup> Janet Ayello,<sup>1</sup> Jeremy M Rosenblum,<sup>1</sup> Mario Marcondes,<sup>6</sup> Mark Currier,<sup>3</sup> Elaine Mardis,<sup>3,4,7</sup> Timothy Cripe ,<sup>4</sup> Dean Lee ,<sup>4</sup> Mitchell S Cairo ,<sup>1,8</sup>

**To cite:** Luo W, Hoang H, Zhu H, et al. Circumventing resistance within the Ewing sarcoma microenvironment by combinatorial innate immunotherapy. *Journal for ImmunoTherapy of Cancer* 2024;12:e009726. doi:10.1136/jitc-2024-009726

► Additional supplemental material is published online only. To view, please visit the journal online (<https://doi.org/10.1136/jitc-2024-009726>).

WL and MSC are joint senior authors.

Accepted 27 August 2024



© Author(s) (or their employer(s)) 2024. Re-use permitted under CC BY-NC. No commercial re-use. See rights and permissions. Published by BMJ.

For numbered affiliations see end of article.

## Correspondence to

Dr Mitchell S Cairo;  
mitchell\_cairo@nymc.edu

## ABSTRACT

**Background** Pediatric patients with recurrent/metastatic Ewing sarcoma (ES) have a dismal 5-year survival. Novel therapeutic approaches are desperately needed. Natural killer (NK) cell number and function are low in ES patient tumors, in large part due to the immunosuppressive tumor microenvironment (TME). Melanoma cell adhesion molecule (MCAM) is highly expressed on ES and associated with ES metastasis. NKTR-255 is a polymer-conjugated recombinant human interleukin-15 (IL-15) agonist improving NK cell activity and persistence. Magrolimab (MAG) is a CD47 blockade that reactivates the phagocytic activity of macrophages.

**Methods** Transcriptome profiling coupled with CIBERSORT analyses in both ES mouse xenografts and human patient tumors were performed to identify mechanisms of NK resistance in ES TME. A chimeric antigen receptor (CAR) NK cell targeting MCAM was engineered by CAR mRNA electroporation into ex vivo expanded NK cells. In vitro cytotoxicity assays were performed to investigate the efficacy of anti-MCAM-CAR-NK cell alone or combined with NKTR-255 against ES cells. Interferon- $\gamma$  and perforin levels were measured by ELISA. The effect of MAG on macrophage phagocytosis of ES cells was evaluated by in vitro phagocytosis assays. Cell-based and patient-derived xenograft (PDX)-based xenograft mouse models of ES were used to investigate the antitumor efficacy of CAR-NK alone and combined with NKTR-255 and MAG in vivo.

**Results** We found that NK cell infiltration and activity were negatively regulated by tumor-associated macrophages (TAM) in ES TME. Expression of anti-MCAM CAR significantly and specifically enhanced NK cytotoxic activity against MCAM<sup>high</sup> but not MCAM-knockout ES cells in vitro, and significantly reduced lung metastasis and extended animal survival in vivo. NKTR-255 and MAG significantly enhanced in vitro CAR-NK cytotoxicity and macrophage phagocytic activity against ES cells, respectively. By combining with NKTR-255 and MAG, the anti-MCAM-CAR-NK cell significantly decreased primary tumor growth and prolonged animal survival in both cell- and PDX-based ES xenograft mouse models.

**Conclusions** Our preclinical studies demonstrate that immunotherapy via the innate immune system by combining tumor-targeting CAR-NK cells with an IL-15 agonist and a CD47 blockade is a promising novel

## WHAT IS ALREADY KNOWN ON THIS TOPIC

⇒ Pediatric solid tumors including Ewing sarcoma are resistant to natural killer (NK) cells due to immunosuppressive tumor microenvironment. Current treatment failed to improve patient outcome for decades. Novel immunotherapy that overcomes the resistance mechanisms is urgently needed.

## WHAT THIS STUDY ADDS

⇒ We identified a novel mechanism of resistance to NK cells in Ewing sarcoma and developed a combinatorial innate immunotherapy combining CAR NK cells with IL-15 agonist and CD47 blockade to overcome multiple resistance mechanisms and enhance anti-tumor efficacy against Ewing sarcoma.

## HOW THIS STUDY MIGHT AFFECT RESEARCH, PRACTICE OR POLICY

⇒ This study suggests that novel combinatorial innate immunotherapy with tumor-targeting CAR NK cells and immunomodulators is a promising therapeutic approach to targeting pediatric solid tumors such as Ewing sarcoma.

therapeutic approach to targeting MCAM<sup>high</sup> malignant metastatic ES.

## INTRODUCTION

Ewing sarcoma (ES) is a malignant pediatric bone and soft tissue tumor. Despite multiple therapeutic approaches including surgery, chemotherapy and radiation over the last 40 years, patients with recurrent metastatic ES have a dismal average 5-year overall survival of less than 30%,<sup>1</sup> largely secondary to therapy resistance within the tumor microenvironment (TME). New therapeutic paradigms are urgently needed and represent an unmet need.<sup>2,3</sup>

Natural killer (NK) cells are innate immune cells highly cytotoxic to tumor cells, including ES.<sup>4</sup> Unlike T cells, NK cells do not require prior sensitization to target tumor cells. NK



function is regulated by a complex balance of inhibitory and activating signals mediated by its inhibitory and activating receptors, respectively.<sup>5</sup> ES cells express high levels of MICA/B, ligands to activating NK receptor NKG2D, and negligible levels of human leukocyte antigen (HLA) class I molecules, ligands to inhibitory NK receptors killer Ig-like receptors (KIRs) of NKG2A.<sup>4,6</sup> These expression patterns shift the balance toward NK cell activation and render ES cells highly sensitive to NK-mediated killing.<sup>4,6</sup>

However, NK cell number and function are low in ES patient tumors, in large part due to the immunosuppressive TME. The mechanisms of TME resistance to NK cell tumor immunity include small numbers of active NK cells, poor NK cell function, activation and persistence, lack of specific targeting, among others.<sup>7</sup> To address low NK cell number and function, our group has developed a genetically engineered feeder cell K562-mbIL-21-4-1BBL to expand peripheral derived NK cells.<sup>8</sup> This approach achieves 35,000 fold expansion of NK cells with high functional activation and preserved telomere length.<sup>8</sup> To further enhance the cytotoxicity of NK cells and facilitate specific targeting of tumor cells, we and others have engineered NK cells to express CARs against cancer targets.<sup>9-12</sup> However, due to the scarcity of tumor-associated antigens in ES,<sup>13</sup> few NK CARs have been developed to target ES. Recently, expression of CAR against the ganglioside antigen GD2 in activated and expanded NK cells has been shown to increase NK cytotoxicity against GD2+ES cells in vitro.<sup>14</sup> However, in the preclinical setting, adoptive transfer of GD2-CAR-NK cells failed to eliminate GD2+ES xenografts.<sup>14</sup> Moreover, the efficacy of CAR-NK cells in limiting ES tumor metastasis is largely uninvestigated. Additional strategies and the development of CAR-NK cells against new cancer targets that are critical in tumor metastatic spread may potentially enhance the antitumor activity of NK cells and circumvent solid tumor resistance.

Melanoma cell adhesion molecule (MCAM) is a cell surface protein overexpressed in common pediatric cancers including ES.<sup>13</sup> MCAM is highly expressed in the embryo but minimally expressed in mature normal tissues.<sup>15</sup> Depletion of MCAM has been shown to inhibit ES cell migration; high MCAM expression is correlated with poor prognosis in ES clinical cohorts.<sup>16</sup> All these features make MCAM a promising target for immunotherapy for patients with metastatic ES. Indeed, a fully humanized antibody targeting MCAM, ABX-MA1 was found to inhibit spontaneous pulmonary metastasis in an orthotopic mouse model of osteosarcoma.<sup>17</sup> However, the anti-tumor effects of MCAM targeted cellular immunotherapy have not been previously investigated in ES.

NK tumor immunity is limited by their poor persistence in vivo. NKTR-255 is an engineered polymer-conjugated recombinant human IL-15 receptor agonist with a high affinity to IL-15R $\alpha$  and a significantly longer half-life compared with natural IL-15 (27 vs <1 hour). NKTR-255 induces the NK cell IL-15 signal transduction pathway (pSTAT5), stimulating NK cell proliferation, survival and cytotoxicity.<sup>18,19</sup> NKTR-255 alone and/or

in combination with various therapeutic monoclonal antibodies are currently under clinical investigations in patients with hematological malignancies (NCT04136756 and NCT03233854) and solid tumors (NCT04616196) as reported by our group and others.<sup>20,21</sup>

TAMs are the most abundant infiltrating immune cells in ES TME<sup>22</sup> and confer a poor prognosis for ES patients.<sup>23</sup> Cross-talks between TAMs and NK cells regulate their functional activities in the TME, resulting in immune activation or suppression.<sup>24</sup> Here, we found that TAMs play a critical role in mediating NK cell resistance in ES. Magrolimab (MAG) is an investigational monoclonal antibody against CD47 that blocks the macrophage “don’t eat me” signal<sup>25</sup> and reactivates macrophage phagocytic and antitumor activities.<sup>26</sup> In the current study, we engineered an ex vivo expanded CAR-NK cell targeting MCAM and combined it with NKTR-255 and MAG to overcome the ES TME resistance to the NK/CAR-NK cell therapy and thereby facilitate increased antitumor efficacy against metastatic ES.

## MATERIALS AND METHODS

Additional methods are detailed in online supplemental materials.<sup>27-31</sup>

### DNA constructs

The MCAM Ab single chain variable fragment (scFv) sequence was generously provided by Bin Liu (University of California at San Francisco)<sup>32</sup> and the scFv DNA (M1) was codon optimized and synthesized (Integrated DNA Technologies), followed by subcloning in frame with a linker (eskygppcpcpm), CD28TM (NP\_001230007.1, aa 34–59), 4-1BB (NP\_001552, aa 213–255), and CD3 $\zeta$  (NP\_000725, aa 52–163) into the pcDNA3 vector to generate a second generation anti-MCAM-CAR. The CAR construct was further optimized by addition of a 2bgUTR.150A sequence generously provided by Carl June and Yangbing Zhao (University of Pennsylvania)<sup>33</sup> at 3' end of the construct. The clustered regulatory interspaced short palindromic repeats (CRISPR)/Cas9 knockout constructs for MCAM were created by cloning the CRISPR guide RNA against MCAM (5'-GTTGCAT-GACCTGAAACGGG-3' (KO1) and 5'-AGGAGGGCG-GCTATCGCTGCG-3' (KO2)) into the lentiCRISPRv2 vector (Addgene plasmid #52961).<sup>34</sup> Guide sequences were designed using the Broad Institute sgRNA designer tool (<https://portals.broadinstitute.org/gpp/public/analysis-tools/sgrna-design>).

### RNA-seq analysis

Total RNA was extracted from tumors using RNeasy mini kit (Qiagen) after homogenization of tumors by GentleMACS tissue dissociator (Miltenyi Biotec) according to manufacturer's instructions. RNA was treated with DNase and RiboZero capture beads (Illumina) to deplete DNA and ribosomal contaminants, respectively. RNA was then used as input for Illumina TruSeq Stranded Total RNA

library preparation kit and sequenced on NovaSeq 6000 to obtain ~60M reads per sample. To prevent any bias that would occur from aligning to one genome at a time, RNA-seq reads were aligned using STAR (STAR\_2.6.1c) to a concatenated reference comprised of the *Homo sapiens* (GRCh38.p12 assembly) and *Mus musculus* (GRCm38. p6 assembly) genomes. The resulting alignments were separated into species-specific bam files, converted back to fastq files and processed through individual human and mouse pipelines, thus creating individual alignments and transcript counts per genome. DESeq2 (V.1.30.1) was used to normalize expression values and to identify differentially expressed genes (DEGs) between groups.<sup>35</sup>

A threshold for DEGs between the two groups was set to an absolute value of fold change  $\geq 1.5$  and a false discovery rate of  $\leq 0.10$ .

### Bioluminescence-based in vitro cytotoxicity assay

Bioluminescence (BLI)-based in vitro cytotoxicity assays were performed as we have previously described<sup>29</sup> with minor modifications. Briefly, luciferase-expressing tumor cells ( $5 \times 10^4$ ) were incubated with effector cells (NK/CAR-NK) at different effector-to-target (E:T) ratios (0.2:1, 0.5:1, and 1:1) in DMEM media supplemented with 10% FBS in 96-well tissue culture plates at 37°C for 4 hours before D-firefly luciferin potassium salt (LUCK-1G, Goldbio, St Louis, Missouri, USA) was added to the cells and BLI was measured with a luminometer (Molecular Devices Multifilter F5 plate reader). In CAR-NK and NKTR-255 combination cytotoxicity assay, MCAM-CAR-NK cells were cultured in RPMI1640 media supplemented with or without NKTR-255 (40 ng/mL, Nektar Therapeutics, San Francisco, California, USA) for 72 hours in the absence of IL-2 before incubating with luciferase-expressing tumor cells.

### Animal studies

All animal studies were performed in accordance with protocols approved by the New York Medical College Institutional Animal Care and Use Committee. Luciferase-expressing A673 cells or ES patient-derived xenograft (PDX) tumors (NCH-EW-1) were implanted into the tibia ( $2 \times 10^5$  cells/site) or flanks (a  $5 \times 5 \times 5$  mm piece/site) of 4–6 weeks old female/male NSG mice (Jackson Laboratory). NSG was used to facilitate stable engraftment of human tumor cells and the evaluation of human NK cell antitumor efficacy. After validation of tumor engraftment by Xenogen In Vivo Imaging System (IVIS) or when PDX tumors reach 5–7 mm in diameter, PBS or NK or CAR-NK were injected ( $1 \times 10^7$  cells/animal, intravenous, once a week for 3–6 weeks) together with or without NKTR-255 (0.3 mg/kg, intravenous, once every 2 weeks) (generously provided by Nektar Therapeutics) and/or MAG (100 µg/animal, i.p. once per day for 12 days) (generously provided by Gilead Sciences, Foster City, California, USA). Before conducting mouse experiments, sample sizes achieving 80% power to detect an effect size  $> 2$  were determined at significant level as 0.05. No randomization

or blinding was used. Tumor growth was monitored by daily caliper measurement and/or weekly IVIS imaging as we have previously described.<sup>36</sup> Mice were followed until death or sacrificed on reaching a tumor size of 1.5 cm in any dimension when the tumors and/or lungs were harvested. For mechanistic study, when xenograft tumors reached 1 cm, Phosphate buffered saline (PBS) or  $1 \times 10^7$  of ex vivo expanded NK cells were injected and tumors were harvested 24 hours after injection and dissected into peripheral (distance from center of the tumor: 3–5 mm) and central (distance from center of the tumor: 0–3 mm) sections for subsequent analyses.

### In vitro phagocytosis assay

Generation of monocyte-derived macrophages was performed as previously reported<sup>37</sup> with minor modifications. Briefly, donor peripheral blood mononuclear cells were isolated by density gradient using Ficoll-Paque PLUS (GE17-1440-03, Millipore sigma) and seeded in RPMI with 10% FBS at a density of  $1 \times 10^7$  cells/mL in 10 cm tissue culture treated plates for 6 days in the presence of 100 ng/mL recombinant human M-CSF (130-096-491, Miltenyi Biotec) with replenishment of media on day 4. ES cells were labeled with CellTracker Green CMFDA dye (C2925, ThermoFisher Scientific) and co-cultured with macrophages at a 2:1 ratio together with or without MAG at a concentration of 1 µg/mL in RPMI for 2–4 hours. Cells were harvested and washed with cold PBS and stained with  $\alpha$ -CD11b (Miltenyi Biotec, 130-110-554). Flow cytometry was carried out and phagocytosis index was measured as the percentage of CD11b+FITC+ macrophages in the total CD11b+macrophages and normalized to the control condition.

## RESULTS

### Characterization of the immune TME of the NK resistant ES tumors

To identify the mechanisms of resistance to NK cells in the ES TME as demonstrated in online supplemental figure 1A, we treated the ES xenograft tumors with ex vivo expanded NK cells or PBS and harvested the tumors 24 hours after treatment. We performed immunostaining (IHC) and found fewer NK cell infiltration into the ES xenograft tumor compared with neuroblastoma xenograft tumor (online supplemental figure 1B). We hypothesized that the immunosuppressive ES TME inhibited NK cell activity and prevented NK cell infiltration into the tumor. To test this hypothesis, we dissected the NK treated and untreated tumors into peripheral and central tumor sections. Total RNA was extracted separately from the NK treated (T) or untreated (U) peripheral (P) or central (C) tumor sections and subjected to transcriptomic sequencing. We identified 1043 murine and 130 human DEGs when comparing treated peripheral (TP) and treated central (TC) tumor samples, 6 murine and 92 human DEGs in comparison of TP and untreated peripheral (UP) samples, and 216 murine and 3 human

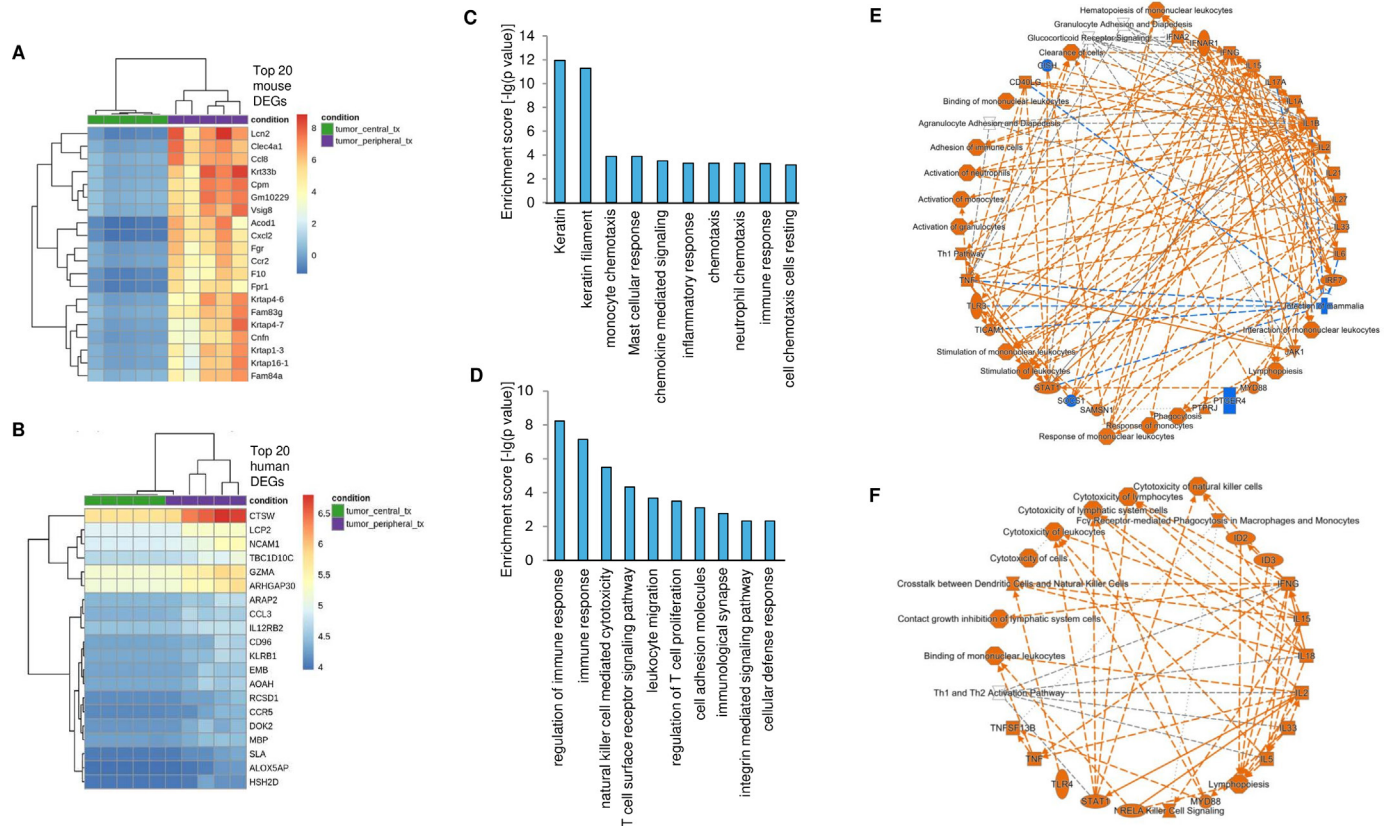


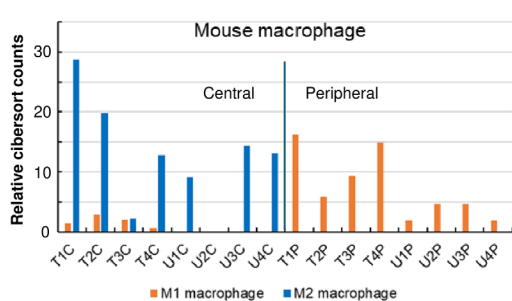
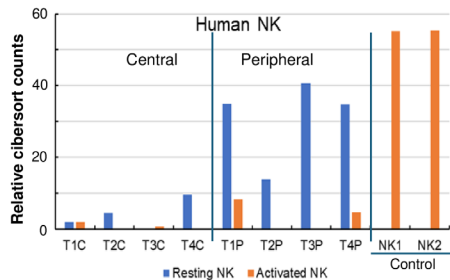
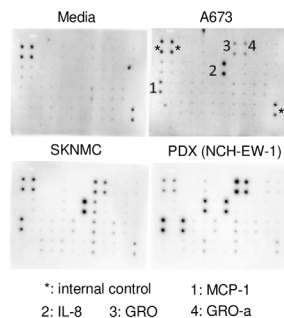
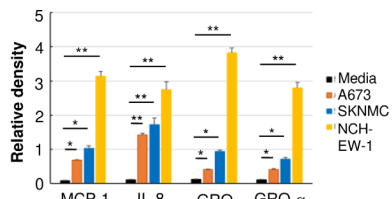
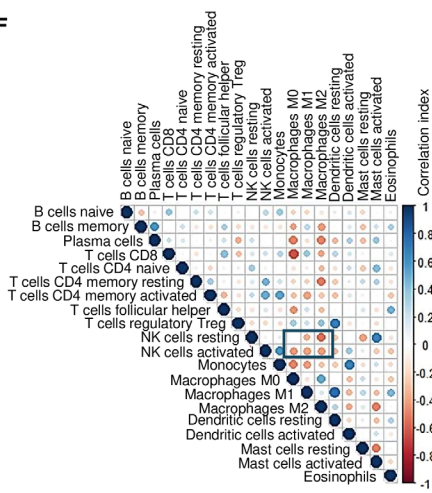
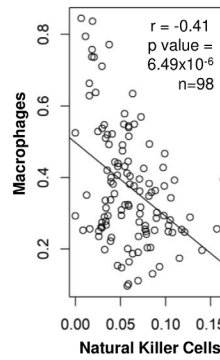
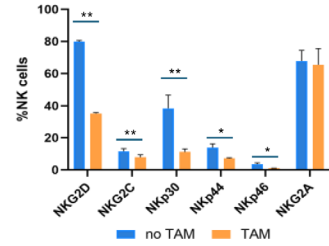
**Figure 1** Identification of mechanisms of resistance to NK therapy in ES xenograft tumors. (A, B) Top differentially expressed murine (A) and human (B) genes comparing NK cell treated peripheral and central tumor sections. ES xenograft tumors (N=5 per condition) were harvested 24 hours after the treatment with PBS or ex vivo expanded NK cells and dissected into peripheral and central tumor sections. Total RNA was extracted from the tumor sections and subjected to RNA-seq and subsequent data analyses for differentially expressed genes. Each cell represents the gene expression of each sample. (C, D) DAVID functional annotation analyses of differentially expressed murine (C) and human (D) genes comparing treated peripheral and central tumor samples. Top functional annotation terms were plotted with enrichment scores ( $-\lg(p\text{ value})$ ). (E, F) Ingenuity pathway analysis of differentially expressed murine (E) and human (F) genes comparing treated peripheral and central tumor samples. Red and blue colors indicate higher and lower expression in treated peripheral tumor samples, respectively. Octagon represents the regulated functions; other shapes indicate the types of molecules. Solid and dash lines represent direct and indirect interactions. DEGs, differentially expressed gene; ES, Ewing sarcoma; NK, natural killer; PBS, phosphate buffered saline.

DEGs comparing TC and UC (untreated central) samples (figure 1A,B, online supplemental figure 2A,B, online supplemental file 1). By DAVID functional annotation analysis using the DEGs between treated (TP and TC) and untreated (UP and UC) samples, we found that immunity, plasma membrane, adaptive immune response, chemotaxis and granzyme-mediated apoptosis signaling pathway are among the most enriched terms in the DEGs of human genes (online supplemental figure 2C), and intermediate filament and keratin are the two most enriched terms in the DEGs of mouse genes (online supplemental figure 2D). Interestingly, using the DEGs between TP and TC samples, we found that the same enriched terms such as keratin/keratin filament and monocyte chemotaxis in the DEG of mouse genes (figure 1C), and regulation of immune response and NK cell-mediated cytotoxicity in the list of human DEGs (figure 1D). This points to a unique immune signature identified only in the peripheral sections of the treated tumors in which NK cells and mouse monocytes play key roles. An ingenuity pathway

analysis (IPA) of the murine and human DEGs further revealed activation of mouse monocytes and crosstalk/interactions between human NK cells and mouse macrophages/monocytes (figure 1E,F).

To further study the ES tumor immune microenvironment, CIBERSORT was used to deconvolute the abundance of immune cell types (online supplemental figure 3A,B). Interestingly, we found that in the peripheral tumor sections, resting instead of activated human NK cells were present, and M1 mouse macrophages were predominant, while in the central tumor sections, M2 mouse macrophages are the most abundant immune cells and human NK cells are barely present (figure 2A,B). All these data suggest that the interaction between mouse macrophages and human NK cells may be part of the mechanism of NK cell resistance in ES.

To investigate which cytokines/chemokines are secreted by the ES cells to attract mouse macrophages, we performed a cytokine array analysis and found that monocyte chemoattractant protein 1 (MCP-1/CCL2), IL-8

**A****B****C****D****F****G****E**

**Figure 2** Macrophages negatively regulate NK cells in the immune microenvironment of Ewing sarcoma (ES) tumors.

(A) Abundance of M1 and M2 mouse macrophages in the peripheral and central sections of ES xenograft tumors. The abundance of mouse immune cells was deconvoluted using RNA-seq gene expression data and Immucell signature matrix by CIBERSORT analysis. The relative counts of M1 (orange) and M2 (blue) macrophages in central and peripheral tumor sections were plotted with each tumor sample. In x-axis sample names, T1C means treated central tumor 1; U1C, untreated central tumor 1; T1P, treated peripheral tumor 1; U1P, untreated peripheral tumor 1. (B) Percentage of resting and activated human NK cells in the peripheral and central tumor sections. RNA-seq gene expression data were used as input matrix and LM22 as signature matrix in CIBERSORT analysis to deconvolute the abundance of human immune cells in the xenograft tumors. The relative counts of resting (blue) and activated (orange) NK cells in central and peripheral tumor sections were plotted with each tumor sample. In x-axis sample names, T1C means treated central tumor 1; T1P, treated peripheral tumor 1. Aliquots of ex vivo expanded NK cells injected into the mice (NK1 and NK2) were used as control samples. (C) Cytokine array analysis for identification of cytokines/chemokines secreted by ES cells and PDX tumor. ES A673 and SKNMC cells and PDX tumor (NCH-EW-1) were cultured in DMEM media for 48 hours before the conditioned media were harvested and assayed by Human Cytokine Antibody Array (Membrane, 42 Targets, Abcam). Fresh DMEM media was used as a negative control. The duplicate black dots at specific positions show positive signals of certain cytokines. Asterisk: internal control; 1: MCP-1/CCL2; 2: IL-8; 3: GRO; and 4: GRO- $\alpha$ . Representative images are shown. The same trend was seen in two independent biological repeats. (D) Quantification of the dot intensity in (C) by ImageJ (<https://imagej.nih.gov/ij/>). Columns represent the relative average density of the dots compared with the internal control. Error bars indicate the SD of duplicate samples in a representative experiment. The same trend was seen in two independent biological repeats. \* $p < 0.05$ , \*\* $p < 0.01$  (two-tailed Student's t-test). (E) Comparison of NK cell receptor expression levels on ex vivo expanded NK cells incubated with or without tumor-associated macrophages (TAMs) isolated from ES xenograft tumors. Macrophages were enriched from the single cell suspension of ES xenograft tumors using the anti-F4/80 MicroBeads (Miltenyi Biotech). Ex vivo expanded NK cells were incubated with (orange) or without (blue) isolated TAMs at a ratio of 1:1 for 4 hours followed by evaluation of NK cell receptor expression via flow cytometry. \* $p < 0.05$ , \*\* $p < 0.01$  (two-tailed Student t-test). Representative results are shown. The same trend was seen in two independent biological repeats. (F) Correlations of immune cells in the TME of ES patient tumors. CIBERSORT analysis was used to deconvolute immune cell composition in ES patient tumors using publicly available ES microarray dataset (GSE17679). CIBERSORT counts were used to analyze the correlations of abundance between various immune cells by Pearson's correlation method. Red and blue dots represent negative and positive correlations, respectively. The darker the color is, the stronger the correlation is. (G) The relative abundance of NK cells and macrophages in individual tumors are represented as open circles in scatterplots. Pearson correlation coefficient  $r = -0.41$  (95% CI  $-0.55$  to  $-0.24$ ),  $p = 6.49 \times 10^{-6}$ . N=98 in GSE17679. PDX, patient-derived xenograft; TME, tumor microenvironment.

and chemokine (C-X-C motif) ligand 1 (CXCL1/GRO/GRO-alpha) are cytokines commonly highly secreted by ES cells (A673 and SKNMC) and PDX tumor (NCH-EW-1) (figure 2C,D). To further investigate whether TAMs directly affect the activity of NK cells, we harvested xenograft tumors from the NSG mice and enriched TAMs from the single cell isolates and incubated them with ex vivo expanded NK cells. Phenotype analyses of NK cells revealed that the expression levels of NK cell activating receptors (NKG2D, NKG2C, NKp30, NKp44, and NKp46) on ex vivo expanded NK cells were significantly decreased after incubation with TAMs (figure 2E). These data suggest that TAMs from the ES xenograft tumors negatively regulate the activity of ex vivo expanded NK cells.

To investigate whether the negative relationship between macrophages and NK cells we observed in the preclinical studies is also present in human ES patient tumors, we performed CIBERSORT analyses to deconvolute immune cell composition in patient TME using a publicly available ES patient tumor microarray dataset (GSE17679, n=98).<sup>30</sup> The correlations between various immune cells were analyzed by Pearson's method. Consistent with our preclinical data, we observed a strong negative correlation among NK cell populations (activated or resting) and macrophage populations (M0, M1, or M2) in the ES patient tumors (figure 2F, red dots represent negative correlations, and figure 2G, Pearson correlation coefficient  $r=-0.41$ ,  $p=6.49\times 10^{-6}$ ). Interestingly, we performed the same CIBERSORT and correlation analyses using neuroblastoma patient tumor RNA-seq dataset (TARGET-NBL, n=155)<sup>31</sup> but did not observe a clear correlation between NK cells and macrophages (online supplemental figure 4).

#### **Expression of anti-MCAM CAR significantly increased cytotoxic activity of NK cells against MCAM<sup>high</sup> ES cells in vitro**

To overcome the resistance in the ES TME and enhance the NK cytotoxic activity and specific targeting of ES cells particularly metastatic ES cells, we engineered ex vivo expanded NK cells to express CAR against MCAM, a novel target that was reported to associate with cancer metastasis.<sup>13-16</sup> We analyzed MCAM expression levels in ES A673, TC32, and SKNMC cells and detected high levels of MCAM expression across all the ES cell lines (figure 3A). We engineered ex vivo expanded NK cells to express CAR directed against MCAM (figure 3B) by CAR mRNA electroporation and found that 78%, 70%, 55% and 39% of NK cells expressed CAR at 1, 2, 4 and 6 days postelectroporation, respectively (figure 3C). We performed NK cytotoxicity assays in vitro using A673, SKNMC, TC32 as target cells and found that, compared with the unmodified expanded NK cells (mock), expression of anti-MCAM CAR in expanded NK cells (CAR) significantly enhanced the NK cytotoxicity against these ES cells at various E:T ratios (0.2:1, 0.5:1, 1:1) (figure 3D). Notably, we observed the significant differences between mock and CAR-NK cells at low E:T ratios likely because of the high sensitivity

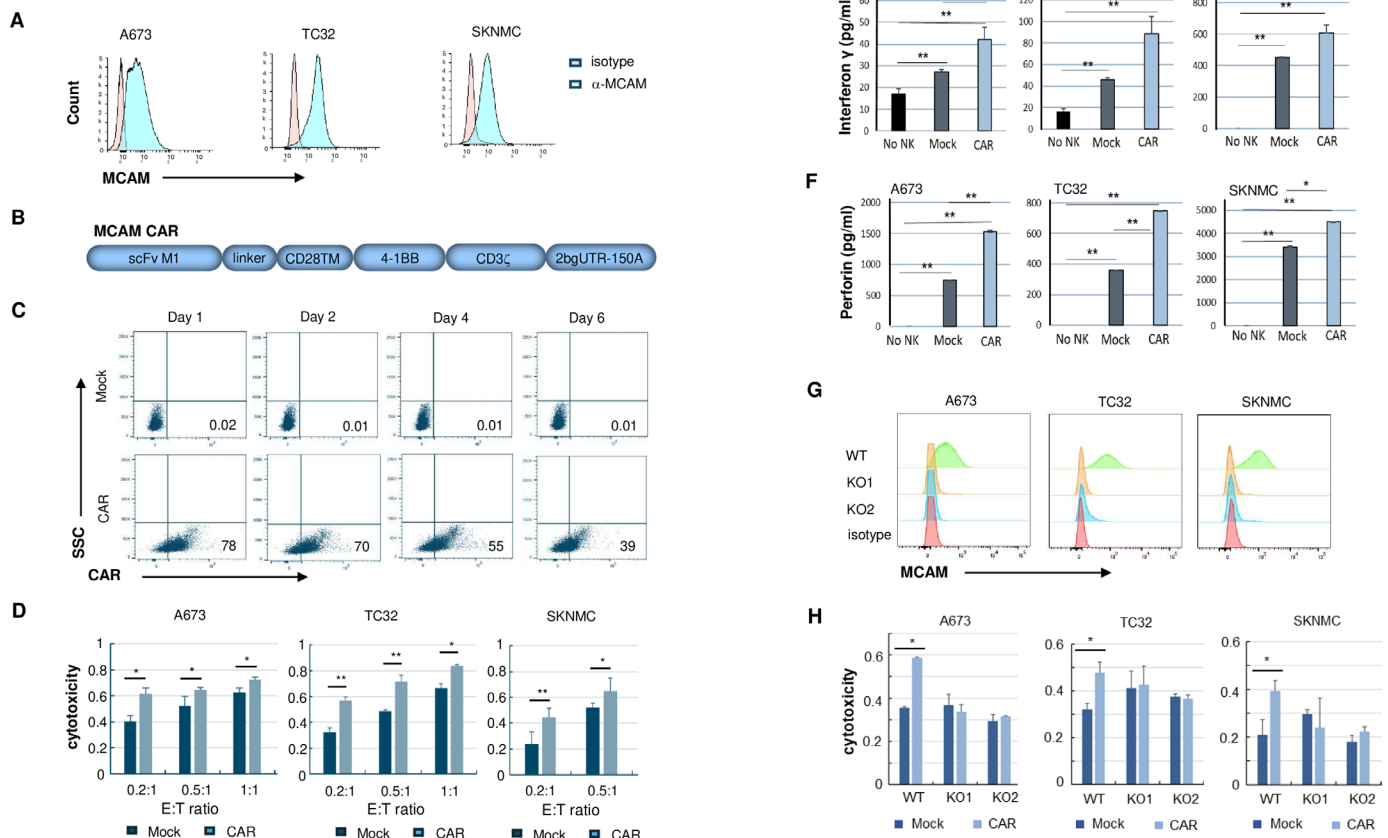
of these tumor cells to NK cells at baseline due to the high expression of NK activating receptor ligands (MIC A/B, CD112, CD155) and low expression of inhibitory receptor ligands (HLA-ABC) on these tumor cells (online supplemental figure 5). Next, we compared mock and CAR-NK cell responses to these tumor cells by quantifying the secretion of cytokines interferon  $\gamma$  (IFN- $\gamma$ ) and perforin and found that CAR-NK cells secreted significantly higher levels of cytokines than mock NK cells when incubated with ES cells (figure 3E,F). To investigate whether the enhanced cytotoxic activity of CAR-NK cells was due to specific targeting of MCAM, we knocked out MCAM in tumor cells by CRISPR/Cas9 (figure 3G) and compared cytotoxic activity of mock and CAR-NK cells against wild-type (WT) and knockout (KO1 and KO2) cells. In the KO tumor cells, we did not observe a significant increase in cytotoxicity with CAR-NK compared with mock NK as we did in the WT tumor cells (figure 3H), demonstrating the increased cytotoxicity of CAR-NK is specific to MCAM<sup>high</sup> tumor cells.

#### **Anti-MCAM-CAR-NK cell significantly decreased lung metastasis and extended animal survival in an ES orthotopic xenograft mouse model**

To evaluate the efficacy of MCAM CAR engineered ex vivo expanded NK cells against ES in vivo, we employed an orthotopic xenograft mouse model of ES metastasis by transplanting luciferase-expressing A673 cells (A673-luc) into the tibia of NSG mice.<sup>36</sup> PBS or mock NK or MCAM-CAR-NK cells were administered via tail vein into the tumor-bearing mice (figure 4A). The frequency of NK/CAR-NK cell injections (once a week) was based on our finding that more than half of the expanded NK cells expressed CAR at day 4 postelectroporation (figure 3C). We found that significantly fewer mice developed lung metastases in the CAR-NK treatment group compared with the PBS control group (43% vs 14%,  $p<0.01$ ) and the mock NK group (28% vs 14%,  $p<0.01$ ) (figure 4B,C). These gave the animals in the CAR-NK group a significant advantage in their survival at day 50 compared with the PBS group (0% vs 50%,  $p<0.05$ ) and the mock NK group (20% vs 50%,  $p<0.05$ ) (figure 4D). Although treatment with mock NK cell also decreased percent of mice with lung metastases compared with the vehicle (43% vs 28%,  $p<0.01$ ), it did not contribute to significantly extended animal survival compared with the control group (figure 4B-D).

#### **NKTR-255 significantly improved NK cell survival, sustained NK expansion and enhanced CAR-NK cell cytotoxicity against ES cells in vitro**

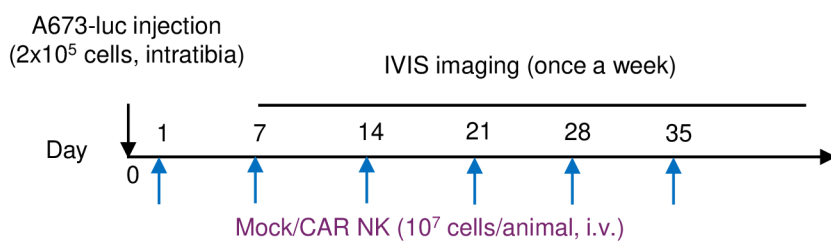
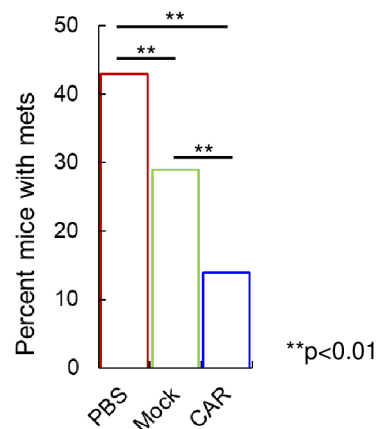
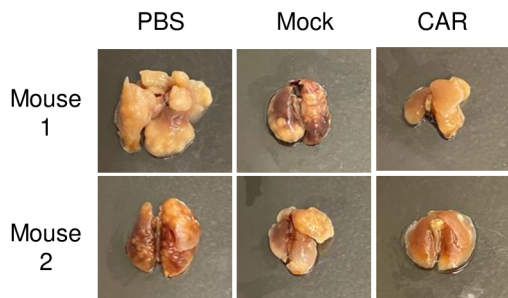
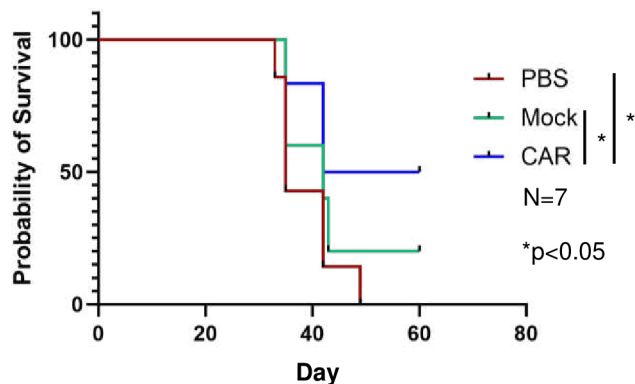
To further enhance the antitumor efficacy of CAR-NK cells and facilitate improved CAR-NK cell survival and durable persistence, we employed a recombinant IL-15 receptor agonist, NKTR-255. We incubated 14-day expanded NK cells with NKTR-255 in the absence of IL-2 and found that NKTR-255 significantly enhanced the expression levels of NKp30, NKG2D and CD94, the



**Figure 3** Expression of anti-MCAM CAR significantly increased cytotoxic activity of NK cells against MCAM<sup>high</sup> ES cells in vitro. (A) Expression of MCAM on ES cells. Cells were stained with isotype or MCAM antibody and subject to flow cytometry analyses. Histograms from a representative experiment were shown. Three biological repeat experiments were performed with similar results (n=3). (B) Schematic representation of the MCAM CAR construct. (C) Electroporation of CAR mRNA resulted in CAR expression on ex vivo expanded NK cells. Two micrograms of CAR mRNA per 10<sup>6</sup> of ex vivo expanded NK cells were used for electroporation using Maxcyte GTx electroporator. CAR expression was detected at 1, 2, 4, 6 days postelectroporation by a biotinylated MCAM protein, followed by FITC-streptavidin staining and flow cytometry analyses. The numbers at the right corner of the dot plots are percent of CAR positive cells. Dot plots from a representative experiment were shown. Three biological repeat experiments (three donors) were performed with similar results. (D) In vitro cytotoxicity of unmodified expanded NK cells (Mock) and anti-MCAM-CAR-NK cells (CAR) against MCAM<sup>high</sup> ES cells A673, TC32, and SKNMC. Mock or CAR-NK cells were incubated with luciferase-expressing ES cells at various effector to target (E:T) ratios (0.2:1, 0.5:1, 1:1) for 4 hours before cytotoxicity was analyzed by addition of D-luciferin to the cells and bioluminescence was measured with a luminometer. Asterisks indicate p<0.05, \*\*p<0.01 (two-tailed Student's t-test). Error bars indicate the SD of triplicate samples in a representative experiment. The same trend was seen in three independent biological repeats. (E, F), Secretion of cytokines IFN- $\gamma$  (E) and perforin (F) from mock and anti-MCAM-CAR-NK cells when incubated with ES cells. Mock or CAR-NK cells were incubated with ES A673, TC32 or SKNMC cells at E:T ratio of 0.2:1 for 4 hours and cytokine secretion in the media was analyzed by ELISA. Tumor cells with no NK cell incubation were used as a negative control. \*p<0.05, \*\*p<0.01 (two-tailed Student's t-test). Error bars indicate the SD of triplicate samples in a representative experiment. The same trend was seen in three independent biological repeats. (G) CRISPR/Cas9 knockout of MCAM in ES cells. MCAM expression in wildtype (WT) and knockout (KO1 and KO2) A673, TC32 and SKNMC cells were detected by flow cytometry using MCAM specific antibody. (H) In vitro cytotoxicity of mock and anti-MCAM-CAR-NK cells against MCAM WT and KO ES cells. Mock or CAR-NK cells were incubated with luciferase-expressing MCAM WT or KO (KO1 and KO2) ES cells (A673, TC32, SKNMC) at E:T ratio of 0.2:1 for 4 hours before cytotoxicity was analyzed by addition of D-luciferin to the cells and bioluminescence was measured with a luminometer. \*p<0.05 (two-tailed Student's t-test). Error bars indicate the SD of triplicate samples in a representative experiment. The same trend was seen in three independent biological repeats. ES, Ewing sarcoma; MCAM, melanoma cell adhesion molecule; NK, natural killer.

NK activating receptors, but not NKG2A or KIR, the NK inhibitory receptors (figure 5A) compared with the non-treated control. Furthermore, NKTR-255 treated NK cells further expanded while the number of non-treated NK cells gradually decreased over time in the absence of IL-2,

demonstrating that NKTR-255 significantly improved NK cell survival and sustained NK expansion in vitro (figure 5B). We next investigated the effect of NKTR-255 on MCAM-CAR-NK cell in vitro cytotoxicity and found that NKTR-255 significantly enhanced the cytotoxic

**A****B****C****D**

**Figure 4** Anti-MCAM-CAR-NK cells significantly decreased lung metastasis and prolonged animal survival in an ES orthotopic xenograft mouse model. (A) Schematic representation of the animal work schedule. Luciferase-expressing A673 cells (A673-luc) were injected into the tibia of NSG mice on day 0. 24 hours later, PBS or mock or CAR-NK cells were administered through tail vein (10<sup>7</sup> cells/animal, once a week for 6 weeks). Tumor growth was monitored by IVIS imaging once a week. (B) Effects of NK/CAR-NK treatment on lung metastasis. Lungs were harvested at the endpoint. Graphs show the percentage of mice with pulmonary lesions in each indicated condition. \*\*Fisher's exact test p<0.01. (C) Representative images of lungs from two of the animals treated with PBS, mock NK, or CAR-NK cells. (D) Kaplan-Meier survival curves for comparison of survival among all groups. Animal survival was followed after therapy initiation using animal death or sacrifice as the terminal event using the Prism program V.8.0 (GraphPad Software). \*p<0.05 (log-rank test). N=7 for each group. ES, Ewing sarcoma; IVIS, In Vivo Imaging System; MCAM, Melanoma cell adhesion molecule; NK, natural killer; PBS, phosphate buffered saline.

activity of MCAM-CAR-NK cells targeting all three lines of ES cells (figure 5C, p<0.05).

#### MAG significantly enhanced macrophage phagocytosis of ES cells *in vitro*

To overcome the suppression of CAR-NK cells by TAMs, we attempted to deplete TAMs by trabectedin which was shown to reduce TAMs while sparing lymphocytes by inducing caspase-8 signaling via the TRAILR2 receptor.<sup>38</sup> However, in our hands, trabectedin induced severe side effects including tail necrosis and weight loss, which resulted in markedly reduced animal survival unrelated to the antitumor efficacy of trabectedin. We next tried to inhibit TAMs by EMAC, a universal macrophage inhibitor and humanized mAb directed against CSF-1R expressed by macrophages.<sup>39 40</sup> Intriguingly, this pan-inhibitor of macrophages combined with CAR-NK and NKTR-255 had minimal effects on decreasing ES xenograft tumor growth, although it depleted mouse macrophages as

evidenced by dramatically decreased mCD45+cells in the animal peripheral blood (online supplemental figure 6A,B).

MAG is a humanized mAb against CD47 that blocks the macrophage “don’t eat me” antiphagocytic signal. Instead of depleting or inhibiting macrophages, MAG reactivates the phagocytic activity of macrophages and converts protumor TAMs into antitumor ones.<sup>41 42</sup> To evaluate the potential of MAG against ES, we investigated and detected high CD47 expression on ES cells (figure 5D) and PDX tumors (figure 5E). We derived macrophages from human peripheral blood monocytes using M-CSF and investigated the *in vitro* phagocytosis of ES cells (labeled with CFMFDA which can be detected by the FITC channel) by macrophages (CD11b+) in the presence of MAG or IgG control using a flow-cytometry-based phagocytosis assay. We found that MAG significantly enhanced the number of macrophages that phagocytosed ES cells

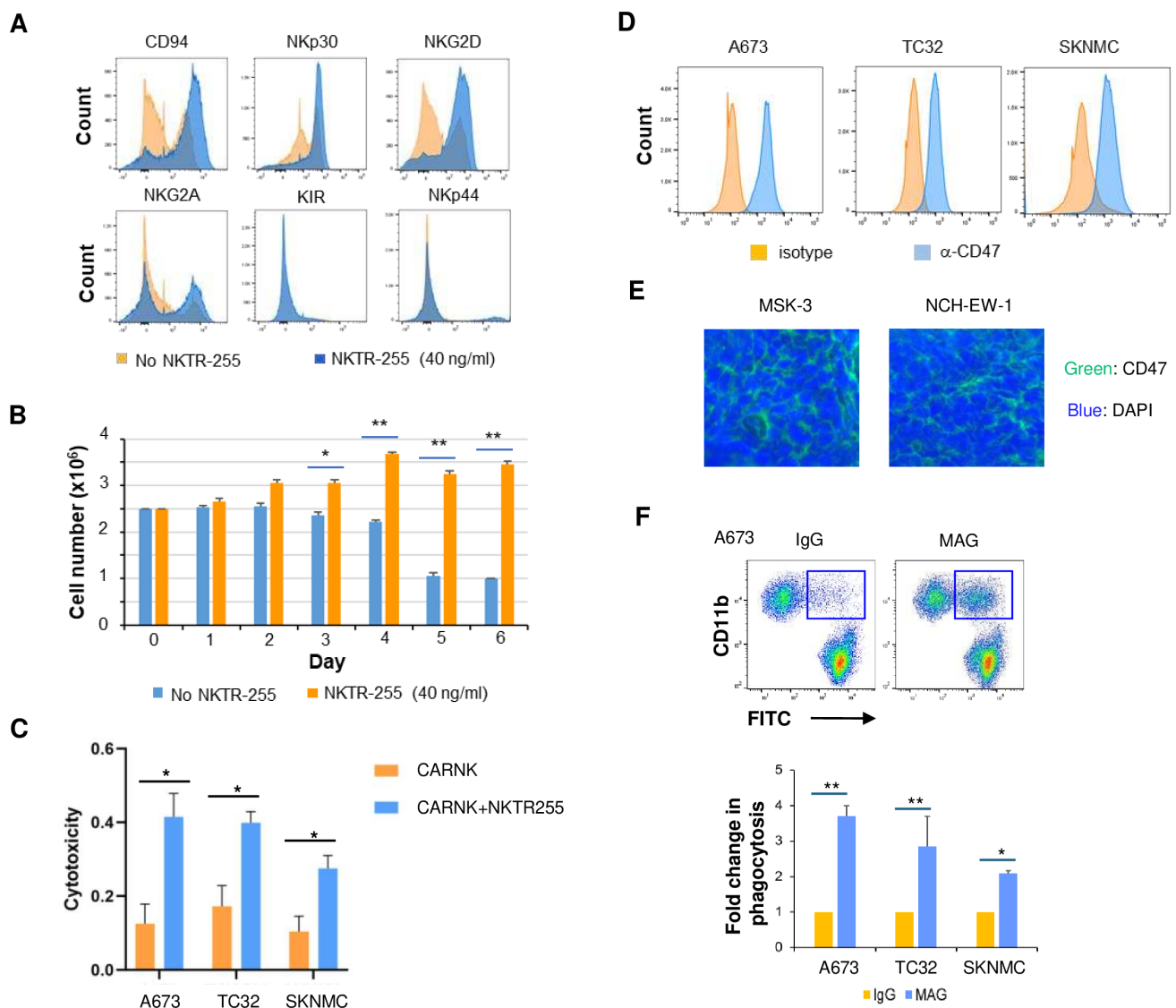


**Figure 5** Effects of NKTR-255 on NK/CAR-NK cells and magrolimab (MAG) on macrophage phagocytosis of Ewing sarcoma (ES) cells in vitro. (A) Effects of NKTR-255 on the expression of NK cell receptors. Ex vivo expanded natural killer (NK) cells were incubated with NKTR-255 (40 ng/mL) for various periods of time (0–6 days) in the absence of IL-2 with replenishment of media and NKTR-255 at day 3. Flow cytometry was performed to detect the expression of NK cell receptors (CD94, NKp30, NKG2D, NKG2A, KIR and NKp44). Representative results from 4 days of incubation were shown. The same trend was seen in three independent biological repeats. (B) Effects of NKTR-255 on NK cell survival and expansion in the absence of IL-2 in vitro. NK cells ( $2.5 \times 10^6$ ) at 14 days of expansion were incubated with NKTR-255 (40 ng/mL) for various periods of time (0–6 days) in the absence of IL-2 with replenishment of media and NKTR-255 at day 3. Viable cells were counted by the method of trypan blue staining. Error bars indicate the SD of triplicate samples in a representative experiment. The same trend was seen in three independent biological repeats. \* $p < 0.05$ , \*\* $p < 0.01$  (two-tailed Student's t-test). (C) In vitro cytotoxic activity of anti-MCAM-CAR-NK cells in combination with NKTR-255 against ES cells. CAR-NK cells were incubated with or without NKTR-255 (40 ng/mL) in the absence of IL-2 for 3 days before incubating with luciferase-expressing ES cells (A673, TC32, SKNMC) at E:T ratio of 0.2:1 for 4 hours. Cytotoxicity was analyzed by addition of D-luciferin and bioluminescent was measured with a luminometer. \* $p < 0.05$ , \*\* $p < 0.01$  (two-tailed Student's t-test). Error bars indicate the SD of triplicate samples in a representative experiment. The same trend was seen in three independent biological repeats. (D) CD47 expression on ES cells. CD47 expression levels were detected by flow cytometry on ES A673, TC32, SKNMC cells. (E) CD47 expression on ES PDX tumors. Immunofluorescent staining by CD47 antibody was performed to detect CD47 (green) expression on MSK-3 and NCH-EW-1 ES PDX tumors. The nuclei were counterstained with DAPI (blue). (F) MAG significantly enhanced macrophage phagocytosis of ES cells. Macrophages were derived from healthy donor peripheral blood mononuclear cells by recombinant human M-CSF (100 ng/mL). ES A673, TC32, SKNMC cells were labeled with CMFDA dye (recognized by FITC channel) and co-cultured with macrophages at a 2:1 ratio together with IgG or MAG (1  $\mu$ g/mL) for 4 hours. Cells were harvested and stained with  $\alpha$ -CD11b followed by flow cytometry analysis. The gated population (CD11b+FITC+) in the dot plots (left) show macrophages phagocytosed ES cells. Right, significantly enhanced macrophage phagocytosis of ES cells (A673, TC32, EWS502) by MAG (blue) compared with IgG control (orange). Quantification of the results in three biological repeats is shown. \* $p < 0.05$ , \*\* $p < 0.01$  (two-tailed Student's t-test). E:T, effector-to-target; PDX, patient-derived xenograft.

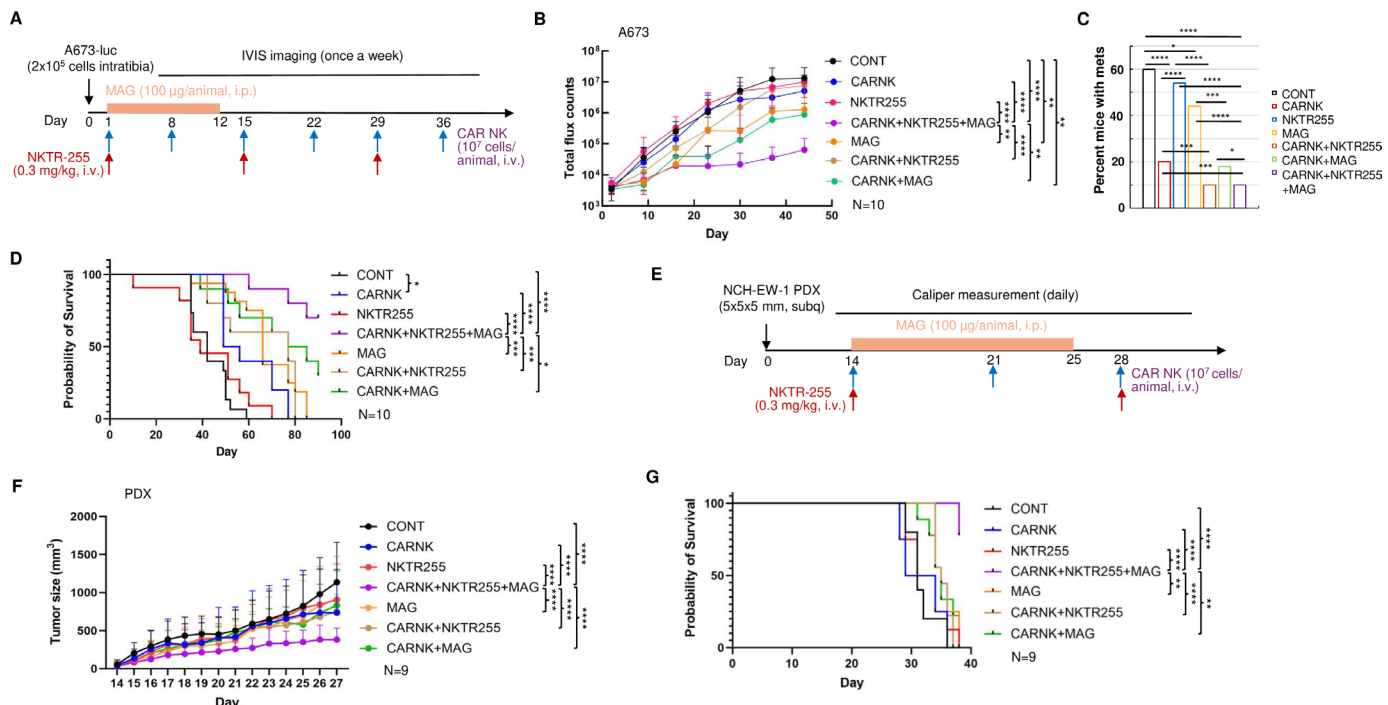


**Figure 6** Combinatorial antitumor effects of anti-MCAM-CAR-NK cells with magrolimab (MAG) and NKTR-255 in ES xenograft mouse models. (A) Schematic representation of the animal work schedule in the cell-based xenograft mouse model. A673-luc cells were injected into the tibia of NSG mice on day 0. 24 hours later, vehicle control or CAR-NK (10<sup>7</sup> cells/animal, i.v., once a week for 6 weeks) or NKTR-255 (0.3 mg/kg, i.v., once every 2 weeks for three times) or MAG (100 µg/animal, i.p., once every day for 12 days) alone or in combination were administered. Tumor growth was monitored by IVIS imaging once a week. (B) Anti-MCAM-CAR-NK cells in combination with NKTR-255 and MAG significantly reduced ES primary xenograft tumor growth in the ES cell-based orthotopic mouse model. Growth rates between groups were analyzed using mixed-effect model. N=10 for each group. Mice were followed until death or sacrificed if any tumor size reached 1.5 cm in any dimension. \*\*p<0.01, \*\*\*p<0.001, \*\*\*\*p<0.0001 (ANOVA). (C) Anti-MCAM-CAR-NK cells in combination with NKTR-255 and MAG significantly reduced lung metastasis. Lungs were harvested at the endpoint. Graphs show the percentage of mice with pulmonary lesions in each indicated condition. \*Fisher's exact test p<0.05, \*\*p<0.01, \*\*\*p<0.001. (D) Anti-MCAM-CAR-NK cells in combination with NKTR-255 and MAG significantly prolonged animal survival of ES xenografted NSG mice. Kaplan-Meier method was used for comparison of survival among all groups. Animal survival was followed after therapy initiation using animal death or sacrifice as the terminal event using the Prism program V.8.0 (GraphPad Software). \*p<0.05 (log-rank test), \*\*p<0.01, \*\*\*p<0.001. N=10 for each group. (E) Schematic representation of the animal work schedule in the PDX mouse model. PDX tumors (NCH-EW-1) were implanted into the flanks of NSG mice. When PDX tumors reach 5–7 mm in diameter (day 14), vehicle control or CAR-NK (10<sup>7</sup> cells/animal, i.v., once a week for 3 weeks) or NKTR-255 (0.3 mg/kg, i.v., once every 2 weeks for twice) or MAG (100 µg/animal, i.p., once every day for 12 days) alone or in combination were administered. Tumor size was measured by caliper every day. (F) Combination of anti-MCAM-CAR-NK cells with NKTR-255 and MAG significantly reduced ES PDX tumor growth. Growth rates between groups were analyzed using mixed-effect model. n=9 for each group. Mice were followed until death or sacrificed if any tumor size reached 1.5 cm in any dimension. \*\*\*\*p<0.0001 (ANOVA). (G) MCAM-CAR-NK cells in combination with NKTR-255 and MAG significantly prolonged animal survival of ES PDX xenografted NSG mice. Kaplan-Meier method was used for comparison of survival among all groups. Animal survival was followed after therapy initiation using animal death or sacrifice as the terminal event using the Prism program V.8.0 (GraphPad Software). \*\*p<0.01 (log-rank test), \*\*\*p<0.001. n=9 for each group. ANOVA, analysis of variance; ES, Ewing sarcoma; i.v., intravenous; MCAM, Melanoma cell adhesion molecule; PDX, patient-derived xenograft.

(FITC+CD11b+) compared with IgG control (figure 5F, p<0.05 and <0.01).

#### Anti-MCAM-CAR-NK cells combined with NKTR-255 and MAG significantly decreased primary tumor growth and prolonged animal survival in ES xenograft mouse models

To test the combination of MCAM-CAR-NK cells with NKTR-255 and/or MAG in vivo, we first used the cell (A673-luc)-based orthotopic mouse model (figure 6A). CAR-NK cells were administered once a week based on our finding that more than half of the expanded NK cells

expressed CAR at day 4 postelectroporation (figure 3C). NKTR-255 and MAG were injected as previously reported with modifications (figure 6A).<sup>19,43</sup> Since MAG is of IgG4 subtype which weakly binds to ADCC effector receptor CD16,<sup>44</sup> we did not include a CAR-NK with IgG control group. We found that CAR-NK and/or NKTR-255 had minimal while MAG alone or combined with CAR-NK had moderate but significant (p<0.01) effects on limiting primary tumor growth compared with the vehicle control. Importantly, combination of CAR-NK with NKTR-255 and

MAG substantially and significantly decreased primary ES xenograft tumor growth compared with vehicle control ( $p<0.0001$ ) or any single agents ( $p<0.01$  vs MAG and  $p<0.0001$  vs CAR-NK or NKTR-255) or any double combinations ( $p<0.01$  vs CAR-NK+MAG and  $p<0.0001$  vs CAR-NK+NKTR-255) (figure 6B). In terms of lung metastasis, CAR-NK cells again significantly decreased the rate of metastasis in the animals compared with the control (20% vs 60%) ( $p<0.0001$ ). While NKTR-255 had no significant effect, combination of NKTR-255 with CAR-NK further significantly decreased the rate of metastasis (55% vs 10%) ( $p<0.0001$ ). We observed a modest but significant (45% vs 60%) ( $p<0.05$ ) effect of MAG on decreasing lung metastasis which was further significantly decreased by combination of CAR-NK (45% vs 18%) ( $p<0.001$ ). Importantly, the animals treated with the combination of the three had one of the lowest rates of lung metastasis (10%) ( $p<0.0001$  vs control or NKTR-255 or MAG,  $p<0.001$  vs CAR-NK,  $p<0.05$  vs CAR-NK+MAG) (figure 6C). The lowest rates of primary tumor growth and lung metastasis together contributed to the highest probability of survival in the triple combination treated animals (70% animals survived at the endpoint) ( $p<0.0001$  vs control or CAR-NK or NKTR-255,  $p<0.001$  vs MAG or CAR-NK+NKTR-255,  $p<0.05$  vs CAR-NK+MAG) (figure 6D). We next extended the in vivo study to a PDX-based ES xenograft mouse model (figure 6E). Due to the limitation in the injection space in tibia, we implanted the NCH-EW-1 PDX tumors in the flanks of NSG mice. We observed no significant difference in primary tumor growth comparing control-treated and single-agent or double-combination-treated animals. This is probably due to the quick development of PDX tumors compared with that of cell-based xenograft tumors, narrowing the therapeutic window of the treatments. Importantly, consistent with what we saw in the cell-based mouse model, the combination of CAR-NK with NKTR-255 and MAG significantly decreased the PDX tumor growth compared with control or any single agents or double combinations ( $p<0.0001$ ) (figure 6F). We could not evaluate the rate of lung metastasis using the PDX model because subcutaneously implanted ES PDX tumors do not metastasize. However, we found that CAR-NK combined with NKTR-255 and MAG significantly extended the probability of animal survival (80% survival at the endpoint) ( $p<0.0001$  vs control or CAR-NK or NKTR-255 or CAR-NK+NKTR-255,  $p<0.01$  vs MAG or CAR-NK+MAG) (figure 6G).

## DISCUSSION

We report here the identification of the negative regulation of NK cells by TAMs as a unique mechanism of resistance to NK cell therapy in a malignant pediatric solid tumor, ES (figures 1 and 2) and the combination of an ex-vivo expanded human CAR-NK cell against a new target, MCAM, an IL-15 agonist, NKTR-255, and a CD47 blockade, MAG, to overcome this resistance (figures 5 and 6). Compared with the mock NK, CAR-NK had

significantly enhanced cytotoxic activity in vitro (figure 3) and significantly reduced lung metastasis and prolonged animal survival in an orthotopic ES model of metastasis (figure 4). Notably, combining CAR-NK cell with NKTR-255 further reduced the rate of metastasis, and CAR-NK cell combined with MAG further decreased primary tumor growth, it took the combination of the three to achieve substantial and significant effects on decreasing both primary and metastatic tumor burden and eventually led to significantly extended animal survival (figure 6). This underscores the necessity of multiple strategies to alter the immunosuppressive TME to circumvent the resistance to innate immune cell therapy in ES. Similar to multiple chemotherapy to treat poor risk ES, it will require a “village” of innate immune cells to circumvent the ES immunosuppressive TME.

Kailayangiri *et al* have previously reported targeting of GD2-expressing ES cells and xenografts with GD2-specific CAR-NK cells.<sup>14</sup> Expression of CAR against GD2 in activated NK cells increased their response to GD2+ES cells in vitro. However, GD2-CAR-NK cells were unable to effectively eliminate ES in xenografts despite high target antigen expression. They subsequently identified moderate to high expression of HLA-G, a ligand to an immune-inhibitory receptor of NK, in GD2-CAR-NK treated tumors as the mechanism of resistance. In our study, based on the RNA-seq data comparing NK treated and untreated peripheral and central ES tumor sections, HLA-G expression was not identified as significantly different among these tumor sections. The discrepancy may be due to different routes of administration of NK cells (intratumoral vs intravenous injections) and timing of harvesting tumor samples for analyses (end of the study vs 24 hours after first treatment) in these two studies. Our RNA-seq data combined with DAVID, IPA, and CIBERSORT analyses indicate that ES tumor cells recruit mouse macrophages to the TME to deactivate functional NK cells and prevent NK cells from infiltrating the tumor. We acknowledge that differences in vascularity of central and peripheral portions of the tumors could have an impact on immune cell tumor infiltration. Nonetheless, the negative regulation of NK cells by TAMs was further supported by our findings that (1) ES tumor cells secrete a high level of MCP-1/CCL2, one of the key chemokines that regulate migration and infiltration of monocytes/macrophages (figure 2C,D), (2) TAMs isolated from the ES xenograft tumors induced decreased expression of NK activating receptors (figure 2E), and (3) alleviation of the negative regulation of NK cells by TAMs using a macrophage-targeting CD47 blockade in part overcame the ES resistance to NK cell therapy (figure 6). Spatial transcriptomics and single-cell RNAseq analyses will be warranted to allow deeper understanding of the role of TAMs in NK cell resistance in ES.

TAM is a well-known key factor in an immunosuppressive TME. Previous reports have shown that TAMs are abundant in ES TME and correlate with poor patient outcomes.<sup>23-25</sup> In the current study, to alleviate the negative

regulation of TAMs to the CAR-NK cells, we attempted targeting TAMs by several approaches including depleting macrophages by trabectedin, inhibiting/depleting macrophages by EMAC and reactivating phagocytic activity of macrophages by MAG. We found that neither trabectedin nor EMAC was an optimal approach to targeting TAMs in ES TME. In comparison, MAG combined with MCAM-CAR-NK and NKTR-255 significantly limited ES xenograft tumor growth and lung metastasis, and significantly extended animal survival (figure 6) without side effects. We speculate that MAG plays an important role in the superior antitumor efficacy of the combinatorial therapy by increasing macrophage phagocytosis of ES cells as supported by our in vitro data (figure 5). Our findings underscored the importance of selectively inhibiting protumor macrophages or reprogramming TAMs toward antitumor subtypes in cancer immunotherapy as previously reported.<sup>46</sup> Although CAR-NK cell combined with NKTR-255 and MAG is effective in decreasing ES tumor growth and metastasis, the animals were not cured, suggesting additional factors contributed to NK cell resistance in the ES TME. These could be immunosuppressive cells in the TME other than TAMs such as MDSCs, regulatory T cells and stromal cells, or tumor cell-derived factors including inhibitory ligands and cytokines such as IL-8 that we identified in the current study (figure 2C,D). Identification and targeting of these factors will be the focus of future investigations.

As in other solid tumors, the mechanisms of resistance to NK cell therapy in ES TME are likely multifactorial as we have previously reported.<sup>7</sup> Additional strategies to improve the NK/CAR-NK cell function, trafficking and tumor targeting will be needed to overcome resistance to NK cell therapy. Cytokines and cytokine analogs such as NKTR-255 can enhance the proliferation, stimulation and persistence of NK cells. NKTR-255 is a polyethylene glycol-conjugate of recombinant hIL-15 which exhibits a longer half-life, reduced clearance and prolonged receptor affinity in comparison to rhIL-15.<sup>19</sup> Functionally, NKTR-255 induces the proliferation and activation of NK and CD8+T cells, increases the CD8+: regulatory T cell ratio, increases the accumulation and persistence of anti-CD19-CAR-T cells in the bone marrow and synergizes with monoclonal antibodies to enhance ADCC in cancer models.<sup>19,47</sup> In addition to cytokines, anti-KIR monoclonal antibodies that block the KIR interactions, histone deacetylase (HDAC) inhibitors that increase the expression of activating NK cell receptors such as NKG2D, as well as bispecific and trispecific NK cell engagers that redirect NK cells to the tumor cells and improve NK cytotoxic potential among others,<sup>7</sup> alone or in combination, are promising approaches under investigation in our group to overcome mechanisms of resistance to NK cell therapy in solid tumors.

In addition to assessing the efficacy of MCAM specific CAR-NK cell therapy against ES primary tumors, we investigated its effects on lung metastasis in an orthotopic ES model of metastasis. We demonstrated that

anti-MCAM-CAR-NK cells alone and in combination with NKTR-255 and MAG significantly decreased lung metastasis in this model (figures 4 and 6A–D). MCAM has long been recognized as a metastasis marker<sup>48</sup> and promotes dissemination of tumor cells in various types of cancer<sup>49–51</sup> including ES.<sup>16</sup> On the other hand, lines of evidence have shown a key role of NK cells in the control of metastatic dissemination.<sup>52</sup> In addition, NK cells prevent metastatic outgrowth by sustaining cancer cell dormancy.<sup>53</sup> In this study, we also observed an inhibitory effect of MAG on ES metastasis, although MAG did not further enhance the already substantial effect of CAR-NK+NKTR-255 on reducing lung metastasis (figure 6C). This suggested a modest anti-metastasis effect of MAG. It was reported that CD47 expression on tumors correlates with tumor metastasis<sup>54</sup>; downregulation or inhibition of CD47, or CD47-blocking antibodies significantly reduced metastasis in cancers such as non-small cell lung cancer<sup>55</sup> and pancreatic ductal adenocarcinoma.<sup>56</sup> By combining the specific and effective targeting of the MCAM<sup>high</sup> disseminated ES cells via anti-MCAM-CAR and the anti-metastasis property of NK cells, coupled with the enhancement of NK in vivo persistence by NKTR-255 and the circumvention of TAMs mediated TME resistance by MAG, we were able to optimize the therapeutic efficacy of NK cell against metastatic ES. Since metastasis is the most important negative prognostic factor in ES, our data suggest that ex vivo expanded anti-MCAM-CAR-NK cells in combination with NKTR-255 and MAG may provide a promising new therapeutic strategy to target metastatic ES and potentially improve patient survival.

Although we demonstrated significant antitumor efficacy of CAR NK combined with NKTR-255 and MAG against ES in vivo, the tumors continued developing, although slower. Deeper and more insightful analyses such as spatial single-cell RNAseq will be helpful in uncovering the mechanisms of resistance to this combinatorial therapy and revealing potential targets to further enhance the antitumor efficacy. Furthermore, approaches to circumventing other core known mechanisms of resistance to NK cell immunotherapy including TGFβ imprinting to overcome TGFβ mediated immunosuppression,<sup>57</sup> CAR NK engineering to enhance migration and tumor infiltration,<sup>58</sup> and development of trispecific NK cell engager (TriKE) to increase the immune synapse between tumor and NK cells and enhance antigen-specific tumor cell killing,<sup>59</sup> among others, may be combined with the CAR-NK+NKTR-255+MAG combinatorial therapy and are under active investigation in our group. Nevertheless, our findings demonstrate that ex vivo expanded MCAM-CAR-NK cells are effective alone but significantly enhanced with combinatorial NKTR-255 and MAG in metastatic ES. Innate immunotherapy induced by CAR-NK cells and macrophages is a promising novel therapeutic approach for poor-risk metastatic pediatric solid tumors such as ES.

**Author affiliations**

<sup>1</sup>Department of Pediatrics, New York Medical College, Valhalla, New York, USA

<sup>2</sup>Department of Pathology, Immunology and Microbiology, New York Medical College, Valhalla, New York, USA

<sup>3</sup>The Steve and Cindy Rasmussen Institute for Genomic Medicine, Columbus, Ohio, USA

<sup>4</sup>Pediatric Hem/Onc/BMT, Nationwide Children's Hospital Hematology Oncology and Blood and Marrow Transplant, Columbus, Ohio, USA

<sup>5</sup>Biomedical Informatics, The Ohio State University, Columbus, Ohio, USA

<sup>6</sup>Nektar Therapeutics, San Francisco, California, USA

<sup>7</sup>Department of Neurosurgery, The Ohio State University, Columbus, Ohio, USA

<sup>8</sup>Departments of Pathology, Immunology and Microbiology, Medicine, Cell Biology and Anatomy, New York Medical College, Valhalla, New York, USA

X Timothy Cripe @kidsoncdoch

**Acknowledgements** The authors would like to thank Bin Liu PhD (University of California San Francisco) for providing the scFv sequence, Carl June MD and Yangbing Zhao MD, PhD (University of Pennsylvania) for providing CAR optimization construct, Nina Slivinsky LVT, RLATG for her technical assistance, Ginny Davenport, RN and Erin Morris, BSN for their great assistance with the preparation of this manuscript.

**Contributors** WL and MSC conceived and designed the study. WL, HH, HZ, KM and XM developed the methodology, performed the analyses and interpreted the data. WL, KM, XM, TC, DL and MSC wrote, reviewed and revised the manuscript. SE, MT, YL, JA, JMR, MM, MC, EM, TC, DL and MSC provided administrative, technical and material support. All authors approved the final manuscript for submission. MSC is the guarantor of the study.

**Funding** This work is supported by funds from the National Cancer Institute Cancer Moonshot U54 CA232561 (TC, DL and MSC), Pediatric Cancer Research Foundation (MSC) and Children's Cancer Fund (MSC).

**Map disclaimer** The inclusion of any map (including the depiction of any boundaries therein), or of any geographic or locational reference, does not imply the expression of any opinion whatsoever on the part of BMJ concerning the legal status of any country, territory, jurisdiction or area or of its authorities. Any such expression remains solely that of the relevant source and is not endorsed by BMJ. Maps are provided without any warranty of any kind, either express or implied.

**Competing interests** MSC has served as a consultant for Jazz Pharmaceuticals, Omeros Pharmaceuticals and Abbvie; Speakers Bureau for Jazz Pharmaceuticals and Sobi; and research funding from Merck, Miltenyi Biotec, Servier, Omeros, Jazz and Janssen. DL reports personal fees and other from Kiadis Pharma, CytoSen Therapeutics, Courier Therapeutics, and Caribou Biosciences outside the submitted work. In addition, DL has a patent broadly related to NK cell therapy of cancer with royalties paid to Kiadis Pharma. TC recently served as a one-time consultant to Blueprint, Incyte, Oncopeptides, DSMB chair for SpringWorks and is a cofounder of Vironexis Biotherapeutics.

**Patient consent for publication** Not applicable.

**Ethics approval** The animal studies were conducted in accordance with the recommendations of the Guide for Care and Use of Laboratory Animals using protocols (#13796) approved by New York Medical College International Animal Care and Use Committee.

**Provenance and peer review** Not commissioned; externally peer reviewed.

**Data availability statement** Data are available on reasonable request. Raw RNA-Seq data are available in GEO (GSE251936). Other data and material are available on reasonable request at mitchell\_cairo@nymc.edu.

**Supplemental material** This content has been supplied by the author(s). It has not been vetted by BMJ Publishing Group Limited (BMJ) and may not have been peer-reviewed. Any opinions or recommendations discussed are solely those of the author(s) and are not endorsed by BMJ. BMJ disclaims all liability and responsibility arising from any reliance placed on the content. Where the content includes any translated material, BMJ does not warrant the accuracy and reliability of the translations (including but not limited to local regulations, clinical guidelines, terminology, drug names and drug dosages), and is not responsible for any error and/or omissions arising from translation and adaptation or otherwise.

**Open access** This is an open access article distributed in accordance with the Creative Commons Attribution Non Commercial (CC BY-NC 4.0) license, which permits others to distribute, remix, adapt, build upon this work non-commercially, and license their derivative works on different terms, provided the original work is

properly cited, appropriate credit is given, any changes made indicated, and the use is non-commercial. See <http://creativecommons.org/licenses/by-nc/4.0/>.

**ORCID iDs**

Timothy Cripe <http://orcid.org/0000-0002-8595-3577>

Dean Lee <http://orcid.org/0000-0001-6693-5392>

Mitchell S Cairo <http://orcid.org/0000-0002-2075-434X>

**REFERENCES**

- 1 Grunewald TGP, Cidre-Aranaz F, Surdez D, et al. Ewing sarcoma. *Nat Rev Dis Primers* 2018;4:5.
- 2 Gaspar N, Hawkins DS, Dirksen U, et al. Ewing Sarcoma: Current Management and Future Approaches Through Collaboration. *J Clin Oncol* 2015;33:3036–46.
- 3 Morales E, Olson M, Iglesias F, et al. Role of immunotherapy in Ewing sarcoma. *J Immunother Cancer* 2020;8:e000653.
- 4 Cho D, Shook DR, Shimasaki N, et al. Cytotoxicity of activated natural killer cells against pediatric solid tumors. *Clin Cancer Res* 2010;16:3901–9.
- 5 Huntington ND, Cursons J, Rautela J. The cancer-natural killer cell immunity cycle. *Nat Rev Cancer* 2020;20:437–54.
- 6 Tong AA, Hashem H, Eid S, et al. Adoptive natural killer cell therapy is effective in reducing pulmonary metastasis of Ewing sarcoma. *Oncimmunology* 2017;6:e1303586.
- 7 Nayyar G, Chu Y, Cairo MS. Overcoming Resistance to Natural Killer Cell Based Immunotherapies for Solid Tumors. *Front Oncol* 2019;9:51.
- 8 Denman CJ, Senyukov VV, Somanchi SS, et al. Membrane-bound IL-21 promotes sustained ex vivo proliferation of human natural killer cells. *PLoS One* 2012;7:e30264.
- 9 Chu Y, Flower A, Cairo MS. Modification of Expanded NK Cells with Chimeric Antigen Receptor mRNA for Adoptive Cellular Therapy. *Methods Mol Biol* 2016;1441:215–30.
- 10 Chu Y, Hochberg J, Yahr A, et al. Targeting CD20+ Aggressive B-cell Non-Hodgkin Lymphoma by Anti-CD20 CAR mRNA-Modified Expanded Natural Killer Cells In Vitro and in NSG Mice. *Cancer Immunol Res* 2015;3:333–44.
- 11 Chu Y, Yahr A, Huang B, et al. Romidepsin alone or in combination with anti-CD20 chimeric antigen receptor expanded natural killer cells targeting Burkitt lymphoma *in vitro* and in immunodeficient mice. *Oncimmunology* 2017;6:e1341031.
- 12 Liu E, Marin D, Banerjee P, et al. Use of CAR-Transduced Natural Killer Cells in CD19-Positive Lymphoid Tumors. *N Engl J Med* 2020;382:545–53.
- 13 Orentas RJ, Yang JJ, Wen X, et al. Identification of cell surface proteins as potential immunotherapy targets in 12 pediatric cancers. *Front Oncol* 2012;2:194.
- 14 Kailayangiri S, Altvater B, Spurny C, et al. Targeting Ewing sarcoma with activated and GD2-specific chimeric antigen receptor-engineered human NK cells induces upregulation of immune-inhibitory HLA-G. *Oncimmunology* 2017;6:e1250050.
- 15 Wang J, Tang X, Weng W, et al. The membrane protein melanoma cell adhesion molecule (MCAM) is a novel tumor marker that stimulates tumorigenesis in hepatocellular carcinoma. *Oncogene* 2015;34:5781–95.
- 16 Sechler M, Parrish JK, Birks DK, et al. The histone demethylase KDM3A, and its downstream target MCAM, promote Ewing Sarcoma cell migration and metastasis. *Oncogene* 2017;36:4150–60.
- 17 McGary EC, Heimberger A, Mills L, et al. A fully human antimelanoma cellular adhesion molecule/MUC18 antibody inhibits spontaneous pulmonary metastasis of osteosarcoma cells *in vivo*. *Clin Cancer Res* 2003;9:6560–6.
- 18 Kuo P, Maiti M, Quach P, et al. Abstract 1603: NKTR-255 engages the IL-15 pathway driving CD8 T cell survival and CD8 memory T cell proliferation. *Cancer Res* 2017;77:1603.
- 19 Miyazaki T, Maiti M, Hennessy M, et al. NKTR-255, a novel polymer-conjugated rhIL-15 with potent antitumor efficacy. *J Immunother Cancer* 2021;9:e002024.
- 20 Shah N, Tan A, Budde E, et al. Safety, tolerability, PK/PD and preliminary efficacy of NKTR-255, a novel IL-15 receptor agonist, in patients with relapsed/refractory hematologic malignancies. *Blood* 2021;138:3134.
- 21 Shah N, Tan A, Budde L, et al. First-in-human phase I study of NKTR-255 in patients with relapsed/refractory hematologic malignancies. *J Immunother Cancer* 2020;8:355.
- 22 Cillo AR, Mukherjee E, Bailey NG, et al. Ewing Sarcoma and Osteosarcoma Have Distinct Immune Signatures and Intercellular Communication Networks. *Clin Cancer Res* 2022;28:4968–82.



- 23 Fujiwara T, Fukushi J, Yamamoto S, et al. Macrophage infiltration predicts a poor prognosis for human ewing sarcoma. *Am J Pathol* 2011;179:1157–70.
- 24 Zhou J, Zhang S, Guo C. Crosstalk between macrophages and natural killer cells in the tumor microenvironment. *Int Immunopharmacol* 2021;101:108374.
- 25 Sallman DA, Al-Malki MM, Asch AS, et al. Magrolimab in Combination With Azacitidine in Patients With Higher-Risk Myelodysplastic Syndromes: Final Results of a Phase Ib Study. *J Clin Oncol* 2023;41:2815–26.
- 26 Chao MP, Weissman IL, Majeti R. The CD47-SIRP $\alpha$  pathway in cancer immune evasion and potential therapeutic implications. *Curr Opin Immunol* 2012;24:225–32.
- 27 Newman AM, Liu CL, Green MR, et al. Robust enumeration of cell subsets from tissue expression profiles. *Nat Methods* 2015;12:453–7.
- 28 Chen Z, Huang A, Sun J, et al. Inference of immune cell composition on the expression profiles of mouse tissue. *Sci Rep* 2017;7:40508.
- 29 Chu Y, Nayyar G, Jiang S, et al. Combinatorial immunotherapy of N-803 (IL-15 superagonist) and dinutuximab with ex vivo expanded natural killer cells significantly enhances in vitro cytotoxicity against GD2 $^+$  pediatric solid tumors and in vivo survival of xenografted immunodeficient NSG mice. *J Immunother Cancer* 2021;9:e002267.
- 30 Savola S, Klami A, Mallykangas S, et al. High Expression of Complement Component 5 (C5) at Tumor Site Associates with Superior Survival in Ewing's Sarcoma Family of Tumour Patients. *ISRN Oncol* 2011;2011:168712.
- 31 Wei JS, Kuznetsov IB, Zhang S, et al. Clinically Relevant Cytotoxic Immune Cell Signatures and Clonal Expansion of T-Cell Receptors in High-Risk MYCN-Not-Amplified Human Neuroblastoma. *Clin Cancer Res* 2018;24:5673–84.
- 32 Bidlingmaier S, He J, Wang Y, et al. Identification of MCAM/CD146 as the target antigen of a human monoclonal antibody that recognizes both epithelioid and sarcomatoid types of mesothelioma. *Cancer Res* 2009;69:1570–7.
- 33 Zhao Y, Moon E, Carpenito C, et al. Multiple injections of electroporated autologous T cells expressing a chimeric antigen receptor mediate regression of human disseminated tumor. *Cancer Res* 2010;70:9053–61.
- 34 Sanjana NE, Shalem O, Zhang F. Improved vectors and genome-wide libraries for CRISPR screening. *Nat Methods* 2014;11:783–4.
- 35 Love MI, Huber W, Anders S. Moderated estimation of fold change and dispersion for RNA-seq data with DESeq2. *Genome Biol* 2014;15:550.
- 36 Luo W, Xu C, Ayello J, et al. Protein phosphatase 1 regulatory subunit 1A in ewing sarcoma tumorigenesis and metastasis. *Oncogene* 2018;37:798–809.
- 37 Rey-Giraud F, Hafner M, Ries CH. In vitro generation of monocyte-derived macrophages under serum-free conditions improves their tumor promoting functions. *PLoS One* 2012;7:e42656.
- 38 Germano G, Frapolli R, Belgiovine C, et al. Role of macrophage targeting in the antitumor activity of trabectedin. *Cancer Cell* 2013;23:249–62.
- 39 Ries CH, Cannarile MA, Hoves S, et al. Targeting tumor-associated macrophages with anti-CSF-1R antibody reveals a strategy for cancer therapy. *Cancer Cell* 2014;25:846–59.
- 40 Ries CH, Hoves S, Cannarile MA, et al. CSF-1/CSF-1R targeting agents in clinical development for cancer therapy. *Curr Opin Pharmacol* 2015;23:45–51.
- 41 Advani R, Flinn I, Popplewell L, et al. CD47 Blockade by Hu5F9-G4 and Rituximab in Non-Hodgkin's Lymphoma. *N Engl J Med* 2018;379:1711–21.
- 42 Sikic BI, Lakhani N, Patnaik A, et al. First-in-Human, First-in-Class Phase I Trial of the Anti-CD47 Antibody Hu5F9-G4 in Patients With Advanced Cancers. *J Clin Oncol* 2019;37:946–53.
- 43 Chao MP, Alizadeh AA, Tang C, et al. Anti-CD47 antibody synergizes with rituximab to promote phagocytosis and eradicate non-Hodgkin lymphoma. *Cell* 2010;142:699–713.
- 44 Rispens T, Huijbers MG. The unique properties of IgG4 and its roles in health and disease. *Nat Rev Immunol* 2023;23:763–78.
- 45 Stahl D, Gentles AJ, Thiele R, et al. Prognostic profiling of the immune cell microenvironment in Ewing's Sarcoma Family of Tumors. *Oncol Immunol* 2019;8:e1674113.
- 46 Mantovani A, Allavena P, Marchesi F, et al. Macrophages as tools and targets in cancer therapy. *Nat Rev Drug Discov* 2022;21:799–820.
- 47 Shah N, Perales M-A, Turtle CJ, et al. Phase I study protocol: NKTR-255 as monotherapy or combined with daratumumab or rituximab in hematologic malignancies. *Future Oncol* 2021;17:3549–60.
- 48 Wu Z, Wu Z, Li J, et al. MCAM is a novel metastasis marker and regulates spreading, apoptosis and invasion of ovarian cancer cells. *Tumour Biol* 2012;33:1619–28.
- 49 Chen Y, Sumardika IW, Tomonobu N, et al. Melanoma cell adhesion molecule is the driving force behind the dissemination of melanoma upon S100A8/A9 binding in the original skin lesion. *Cancer Lett* 2019;452:178–90.
- 50 Lei X, Guan C-W, Song Y, et al. The multifaceted role of CD146/MCAM in the promotion of melanoma progression. *Cancer Cell Int* 2015;15:3.
- 51 Zoni E, Astrologo L, Ng CKY, et al. Therapeutic Targeting of CD146/MCAM Reduces Bone Metastasis in Prostate Cancer. *Mol Cancer Res* 2019;17:1049–62.
- 52 López-Soto A, Gonzalez S, Smyth MJ, et al. Control of Metastasis by NK Cells. *Cancer Cell* 2017;32:135–54.
- 53 Correia AL, Guimaraes JC, Auf der Maur P, et al. Hepatic stellate cells suppress NK cell-sustained breast cancer dormancy. *Nature New Biol* 2021;594:566–71.
- 54 Yuan J, He H, Chen C, et al. Combined high expression of CD47 and CD68 is a novel prognostic factor for breast cancer patients. *Cancer Cell Int* 2019;19:238.
- 55 Zhao H, Wang J, Kong X, et al. CD47 Promotes Tumor Invasion and Metastasis in Non-small Cell Lung Cancer. *Sci Rep* 2016;6:29719.
- 56 Michaels AD, Newhook TE, Adair SJ, et al. CD47 Blockade as an Adjuvant Immunotherapy for Resectable Pancreatic Cancer. *Clin Cancer Res* 2018;24:1415–25.
- 57 Foltz JA, Moseman JE, Thakkar A, et al. TGF $\beta$  Imprinting During Activation Promotes Natural Killer Cell Cytokine Hypersecretion. *Cancers (Basel)* 2018;10:423.
- 58 Kremer V, Ligtenberg MA, Zendehdel R, et al. Genetic engineering of human NK cells to express CXCR2 improves migration to renal cell carcinoma. *J Immunother Cancer* 2017;5:73.
- 59 Vallera DA, Oh F, Kodal B, et al. A HER2 Tri-Specific NK Cell Engager Mediates Efficient Targeting of Human Ovarian Cancer. *Cancers (Basel)* 2021;13:3994.